Contribution from the Departments of Inorganic and Organic Chemistry, The University of Sydney, NSW 2006, Australia

Effect of Electrolyte Concentration on Axial Anion Ligation in Manganese(III) *meso*-Tetraphenylporphyrin Chlorides[1]

Garry J. Foran,[†] Robert S. Armstrong,*[,†] Maxwell J. Crossley,[‡] and Peter A. Lay[†]

Received July 17, 1991

The ionic strength dependence of axial ligation in manganese(III) 5,10,15,20-tetraarylporphyrin chlorides has been investigated and found to be much more important than has hitherto been recognized. In this study tetrahydrofuran solutions of the metalloporphyrin, 0.0–0.5 M in the electrolyte tetrabutylammonium tetrafluoroborate, were examined by electronic absorption and resonance Raman spectroscopies as well as ultramicroelectrode voltammetry. The metalloporphyrin complexes were found to be significantly dissociated even at moderate electrolyte concentrations. In all cases, anion dissociation was promoted as concentration of electrolyte was increased. The fully dissociated analogues were independently generated by reaction of the manganese(III) porphyrin with $AgBF_4$. Tentative assignments for the low-wavenumber region of the resonance Raman spectra of the studied complexes are made and solution structures inferred.

Introduction

Manganese porphyrins have several interesting aspects of their physical and chemical properties which distinguish them from other metalloporphyrins. Their electronic absorption spectra are atypical.[2] They also have a number of interesting chemical properties, including their reactions with dioxygen,[3] photolytic redox reactions,[4-6] and the dependency of redox potentials on a coordinated ligand.[7-9] In addition, the electron-transfer kinetics of the manganese porphyrins have been studied because they exhibit behavior significantly different from that of analogous iron and cobalt systems.[10-14]

The weak axial binding observed in manganese(III) porphyrins has been well established and reported.[8,15,16] The chemical effects of this phenomenon have continued to arouse interest with much recent work on manganese(III) porphyrins focusing on axial ligation.[17,18] The possibility of solution ionic strength influencing the degree of axial ligation in manganese(III) 5,10,15,20-tetraarylporphyrins has been noted previously,[8] but specific measurements have not been reported.

Unlike many other metalloporphyrins, manganese porphyrins lend themselves well to a study of the immediate metal environment owing to the highly structured nature of their resonance Raman (RR) spectra in the low-wavenumber region.[19-23] The vibrational modes observed in this region include axial-ligand-dependent modes,[19,21] modes attributable to vibrations of the phenyl groups, and out-of-plane vibrations of the porphyrin skeleton. The axial-ligand-dependent modes are particularly useful in a study of the immediate metal environment. The out-of-plane modes are also convenient probes of molecular and electronic structure.[24,25]

Electrochemical studies on the redox properties of porphyrins and metalloporphyrins are numerous, and recently ultramicroelectrodes have been used in these studies.[26] Manganese(III) porphyrins have been studied by electrochemical methods in the fields of electron-transfer kinetics and ligand addition reactions,[10-13] counterion and solvent effects,[7-9] and porphyrin substituent effects.[28] In the present study, some of the special properties of ultramicroelectrodes[26,27,29,30] have been employed to conduct voltammetric experiments over a range of electrolyte concentrations in a highly resistive medium, namely in tetrahydrofuran solutions. Such experiments have not been reported previously for manganese porphyrins, and the results presented here provide important information for the interpretation of electrochemical data obtained using conventionally sized electrodes.

In this work, RR spectroscopy, ultramicroelectrode voltammetry, and electronic absorption spectroscopy have been used to probe the effect of increasing electrolyte concentration on axial ligation in a series of substituted manganese(III) 5,10,15,20-tetraarylporphyrin chlorides (**1a–d**). It has been found that the effect is much more significant than has been recognized hitherto.

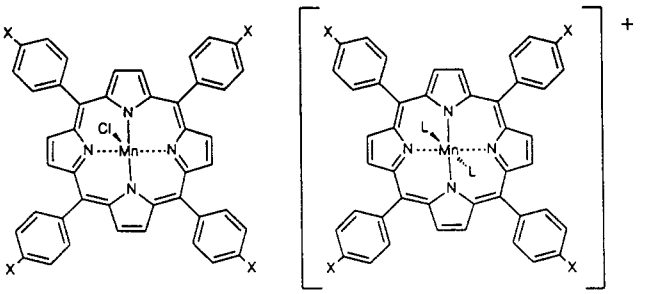

1a X = H
1b X = OMe
1c X = Cl
1d X = CN

2a X = H
2b X = OMe
2c X = Cl
2d X = CN

[†] Department of Inorganic Chemistry.
[‡] Department of Organic Chemistry.

(1) Reported in part previously: Armstrong, R. S.; Foran, G. J.; Lay, P. A. *Abstracts of Papers*, XI International Conference on Raman Spectroscopy, London, U.K.; John Wiley and Sons: Chichester, U.K., 1988; Abstract 10.30, 587. Foran, G. J.; Armstrong, R. S.; Lay, P. A.; Crossley, M. J. *Abstracts of Papers*, XXVII International Conference on Coordination Chemistry, Broadbeach, Queensland, Australia; 1989; Abstract W36.
(2) Gouterman, M. In *The Porphyrins*; Dolphin, D., Ed.; Academic Press: New York, 1982; Vol. III, p 1.
(3) Hoffman, B. M.; Weschler, C. J.; Basolo, F. *J. Am. Chem. Soc.* **1976**, *98*, 5473. Jones, R. D.; Summerville, D. A.; Basolo, F. *J. Am. Chem. Soc.* **1978**, *100*, 4416.
(4) Harriman, A. *J. Chem. Soc., Dalton Trans.* **1984**, 141.
(5) Jin, T.; Suzuki, T.; Imamura, T.; Fujimoto, M. *Inorg. Chem.* **1987**, *26*, 1280.
(6) Takahashi, K.; Komura, T.; Imanaga, H. *Bull. Chem. Soc. Jpn.* **1983**, *56*, 3203.
(7) Boucher, L. J.; Garber, H. K. *Inorg. Chem.* **1970**, *9*, 2644.
(8) Kelly, S. L.; Kadish, K. M. *Inorg. Chem.* **1982**, *21*, 3631.
(9) Iwaizumi, M.; Komuro, H. *Inorg. Chim. Acta* **1986**, *111*, L9.
(10) Kadish, K. M.; Sweetland, M.; Cheng, J. S. *Inorg. Chem.* **1978**, *17*, 2795.
(11) Kadish, K. M.; Kelly, S. *Inorg. Chem.* **1979**, *18*, 2968.
(12) Kelly, S.; Lancon, D.; Kadish, K. M. *Inorg. Chem.* **1984**, *23*, 1451.
(13) Bettelheim, A.; Ozer, D.; Weinraub, D. *J. Chem. Soc., Dalton Trans.* **1986**, 2297.
(14) Kadish, K. M. In *Iron Porphyrins*; Lever, A. B. P., Gray, H. B., Eds.; Addison-Wesley Publishing Co.: Reading, MA, 1983.
(15) Boucher, L. J. *Ann. N.Y. Acad. Sci.* **1973**, *205*, 409.
(16) Boucher, L. J. *Coord. Chem. Rev.* **1972**, *7*, 289.
(17) Williamson, M. M.; Hill, C. L. *Inorg. Chem.* **1987**, *26*, 4155.
(18) Parthasarathi, N.; Spiro, T. G. *Inorg. Chem.* **1987**, *26*, 2280.
(19) Gaughan, R. R.; Shriver, D. F.; Boucher, L. J. *Proc. Natl. Acad. Sci. U.S.A.* **1975**, *72*, 433.
(20) Shelnutt, J. A.; O'Shea, D. C.; Yu, N.; Cheung, L. D.; Felton, R. H. *J. Chem. Phys.* **1976**, *64*, 1156.
(21) Asher, S.; Sauer, K. *J. Chem. Phys.* **1976**, *64*, 4115.
(22) Campochiaro, C.; Hofmann, J. A.; Bocian, D. F. *Inorg. Chem.* **1985**, *24*, 449.
(23) Czernuszewicz, R. S.; Su, Y. O.; Stern, M. K.; Macor, K. A.; Kim, D.; Groves, J. T.; Spiro, T. G. *J. Am. Chem. Soc.* **1988**, *110*, 4158.

0020-1669/92/1331-1463$03.00/0 © 1992 American Chemical Society

Experimental Section

Porphyrins. Chloro(5,10,15,20-tetraphenylporphinato(2−))manganese(III) (**1a**), chloro(5,10,15,20-tetrakis(4-methoxyphenyl)porphinato(2−))manganese(III) (**1b**), chloro(5,10,15,20-tetrakis(4-chlorophenyl)porphinato(2−))manganese(III) (**1c**), and chloro(5,10,15,20-tetrakis(4-cyanophenyl)porphinato(2−))manganese(III) (**1d**), henceforth abbreviated as [Mn(TPP)Cl], [Mn(T(4-OCH_3P)P)Cl], [Mn(T(4-ClP)P)Cl], and [Mn(T(4-CNP)P)Cl], respectively were prepared by metalation of the corresponding free base porphyrins using manganese acetate followed by anion exchange in the usual way.[8,19] The fully anion-dissociated compounds **2a–d** were synthesized by weighing a stoichiometric excess of $AgBF_4$ into a sample tube or volumetric flask and then adding a THF solution of the relevant porphyrin under inert atmosphere. Given the porphyrin concentration used (~0.25 mM), the amount of colloidal silver chloride thus generated was so small as to make filtration unnecessary. Isotopically substituted [Mn(TPP)^{37}Cl] was made by employing a solution of $Na^{37}Cl$ (95.6 atom %, Isotec, Inc.) during the anion exchange of [Mn(TPP)acetate].

Materials and Solutions. Tetrabutylammonium tetrafluoroborate ($Bu_4N^+BF_4^-$) was synthesized according to the method of Rehan et al.[31] except for the recrystallization step. This step was performed at room temperature by dissolving the crude electrolyte in a minimum volume of ethyl acetate. The solution was then filtered and the product crystallized by the addition of about three equivalent volumes of diethyl ether. After filtration the pure $Bu_4N^+BF_4^-$ was washed several times with diethyl ether and allowed to dry thoroughly before being stored over P_4O_{10}. Silver tetrafluoroborate (98%, $AgBF_4$) was used as received from Aldrich Chemicals. Tetrahydrofuran (extra pure grade, Merck) was dried over sodium wire and then distilled in the presence of benzophenone ketal under argon immediately before use.[32]

Resonance Raman Spectroscopy. RR spectra were obtained with Ar^+ (476.5 nm) laser excitation. The samples were spun in a cylindrical quartz cell in 90° scattering geometry. With a f1.0 collection lens the scattered light was focused onto the slits of a ISA/Jobin-Yvon U1000 double monochromator equipped with an RCA 31034 photomultiplier tube and photon-counting electronics. The data were collected digitally and stored with an IBM compatible AT microcomputer using ISA/Jobin-Yvon Enhanced Prism software. Sample concentrations were typically in the range 0.25–1 mM.

Electrochemistry. The porphyrin electrochemistry was characterized using a Bioanalytical Systems (BAS) 100 electrochemical analyzer, interfaced with an Osborne PC Executive microcomputer for data storage and retrieval. When work was done with ultramicroelectrodes, either a Keithley 485 autoranging picoammeter[30] or a signal preamplifier (built in-house) was employed. The experiments were carried out inside an aluminum Faraday cage that was purged with house nitrogen throughout. The ultramicroelectrodes consisted of a 10-μm gold wire, sealed inside a glass sheath, the end of which was ground down to give a microdisc electrode. Immediately prior to use, the electrode was polished with diamond pastes (Buehler Ltd.) to 0.25-μm smoothness. Before each scan the electrode was polished with an aqueous slurry of 0.1-μm alumina (Struers), rinsed with THF, and then sonicated in THF. Conventional electrochemistry was carried out using a gold disk electrode of approximately 1-mm diameter. The electrochemical techniques used were linear sweep voltammetry (LSV) and cyclic voltammetry (CV). To measure the half-wave potentials using LSV, the potential range was scanned at relatively slow scan rates (i.e. ≤100 mV s^{-1}) to ensure steady-state or near-steady-state behavior. The potential at which the second derivative of the resulting voltammogram was equal to zero was taken as $E_{1/2}$. To ensure that $E_{1/2}$ was not shifting due to iR drop, the potential range was scanned in both a cathodic and anodic direction and the average of the half-wave potentials thus obtained was calculated. In the case of CV, the midpoint of the cathodic and anodic peak potentials was taken to be $E_{1/2}$. A Ag/AgCl/KCl(saturated) reference electrode (BAS) was used throughout and all electrochemical potentials were measured relative to the ferrocenium/ferrocene (Fc^+/Fc) redox couple. The potential of the Fc^+/Fc couple was measured by adding ferrocene (Fluka) either to the sample cell after $E_{1/2}$ for the porphyrin had been measured or to a pure electrolyte solution. No difference was observed between these two procedures at a given concentration of electrolyte. Sample concentrations were the same as for the RR experiments with all solutions being degassed with argon (CIG, high-purity grade) for a minimum of 10 min prior to measurements being taken. The argon was further purified before use by bubbling it through a Cr(II) solution and then through concentrated H_2SO_4. When using the 1-mm gold disk electrode, 100% iR compensation was employed.

Electronic absorption spectra were recorded on a Cary 17D spectrophotometer with the data being stored digitally via a Commodore PET microcomputer.

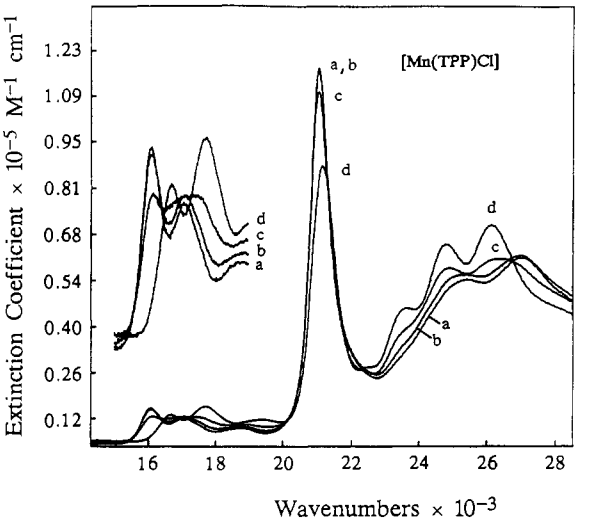

Figure 1. Effect of increasing [$Bu_4N^+BF_4^-$] and chloride extraction on the electronic absorption spectrum of [Mn(TPP)Cl] in THF. Concentrations of $Bu_4N^+BF_4^-$ are (a) 0 M, (b) 0.1 M, and (c) 0.5 M. (d) is the spectrum resulting from treating a neat THF solution of [Mn(TPP)Cl] with $AgBF_4$.

Results

Electronic Absorption Spectroscopy. The electronic absorption spectra of the four manganese(III) porphyrins (**1a–d**) were recorded over the range 350–700 nm in neat THF and at background electrolyte ($Bu_4N^+BF_4^-$) concentrations of ~0.1 and ~0.5 M. With adoption of the numbering system of Boucher,[16] there are the porphyrin Q bands (III and IV) at approximately 16 000–17 000 cm^{-1}, the dominant dual character band V is at about 21 000 cm^{-1}, and the strongly absorbing bands Va and VI are at about 25 000 and 27 000 cm^{-1}, respectively. A summary of peak positions and molar extinction coefficients in neat THF is given in Table I. The effect of increasing concentration of electrolyte in the visible spectrum is greatest in the region of bands V, Va, and VI. While band V loses intensity and is slightly shifted to higher energy, bands Va and VI gain some intensity and shift to lower energy. Further, a new transition appears as a shoulder on the low-energy side of band Va. Hereafter, this transition will be referred to as band Vb. A summary of the effect of increasing electrolyte concentration on the positions and intensities of the absorption maxima is given also in Table I. While the peripheral phenyl substituents only vary slightly the positions of the electronic absorption bands, there is a general trend toward higher energy with increased electron-withdrawing capacity of the phenyl substituent. That is the positions of corresponding bands through the series **1a–d** vary as follows:

$$\mathbf{1b < 1a < 1c < 1d}$$

A study of Table I reveals that the methoxyphenyl-substituted porphyrin is most sensitive to a variation in [$Bu_4N^+BF_4^-$]. The spectral changes for compound **1a** as a function of the concentration of [$Bu_4N^+BF_4^-$] are shown in Figure 1.

The visible spectra of the metalloporphyrins in which the axial chloride has been removed by addition of Ag^+ (compounds **2a–d**) show a further progression of the changes observed with increasing [$Bu_4N^+BF_4^-$] (see Table I and Figure 1). The spectra still exhibit

(24) Choi, S.; Spiro, T. G. *J. Am. Chem. Soc.* **1983**, *105*, 3683.
(25) Czernuszewicz, R. S.; Li, X.; Spiro, T. G. *J. Am. Chem. Soc.* **1989**, *111*, 7024.
(26) Baer, C. D.; Camaioni-Neto, C. A.; Sweigart, D. A.; Bond, A. M.; Mann, T. F.; Tondreau, G. A. *Coord. Chem. Rev.* **1989**, *93*, 1.
(27) Geng, L.; Murray, R. W. *Inorg. Chem.* **1986**, *25*, 3115.
(28) Kadish, K. M.; Morrison, M. M. *Bioinorg. Chem.* **1977**, *7*, 107.
(29) Heinze, J. *Ber. Bunsen-Ges. Phys. Chem.* **1981**, *85*, 1096.
(30) Bond, A. M.; Lay, P. A. *J. Electroanal. Chem. Interfacial Electrochem.* **1986**, *199*, 285.
(31) Rehan, A. E.; Barkhau, R. A.; Williams, J. M. In *Inorganic Syntheses*; Shreeve, J. M., Ed.; John Wiley and Sons: New York, 1986; Vol 24, p 139.
(32) Allen, G. Ph.D. Thesis, University of Sydney, 1990.

Table I. Electronic Absorption Band Maxima and Intensities of the Manganese(III) Tetraphenylporphyrin Chlorides in THF Solution at Various Concentrations of Tetrabutylammonium Tetrafluoroborate ($Bu_4N^+BF_4^-$) and after Treatment with Silver Tetrafluoroborate ($AgBF_4$)

electronic abs band	concn of $Bu_4N^+BF_4^-$/M			
	0	0.10	0.50	0.10 + $AgBF_4$
		[Mn(TPP)Cl]		
III	16.07[a] (1.20)[b]	16.07 (1.20)	16.18 (0.893)	16.70 (1.00)
IV	17.07 (1.00)	17.07 (0.964)	17.33 (1.00)	17.73 (1.32)
V	21.10 (11.39)	21.10 (11.46)	21.13 (10.64)	21.17 (8.54)
Va	25.39 (4.93)	25.39 (5.14)	25.02 (5.29)	24.80 (6.02)
Vb			23.65 (3.39)	23.65 (4.04)
VI	27.05 (5.44)	27.05 (5.62)	26.50 (5.44)	26.13 (6.57)
		[Mn(T(4-OCH_3P)P)Cl]		
III	15.92 (1.50)	15.95 (1.42)	15.99 (1.30)	16.44 (1.43)
IV	17.03 (0.96)	17.03 (1.00)	17.17 (1.09)	17.47 (1.35)
V	20.95 (12.54)	20.95 (10.86)	20.95 (10.53)	20.95 (8.87)
Va	24.72 (5.60)	24.72 (5.10)	24.72 (5.10)	24.72 (7.04)
Vb			23.21 (4.01)	23.21 (6.26)
VI	26.72 (5.68)	26.72 (5.10)	26.31 (5.01)	25.87 (7.66)
		[Mn(T(4-ClP)P)Cl]		
III	16.10 (1.15)	16.13 (1.07)	16.16 (1.02)	16.71 (0.75)
IV	17.10 (1.00)	17.25 (1.00)	17.25 (1.00)	17.77 (1.07)
V	21.06 (10.17)	21.10 (10.07)	21.13 (10.07)	21.28 (8.52)
Va	25.57 (4.87)	25.42 (4.87)	25.27 (4.87)	24.88 (5.66)
Vb				23.67 (3.62)
VI	27.12 (5.41)	27.06 (5.37)	27.00 (5.23)	26.21 (6.00)
		[Mn(T(4-CNP)P)Cl]		
III	16.12 (1.04)	16.18 (1.10)	16.24 (0.89)	16.78 (0.84)
IV	17.15 (0.95)	17.18 (1.07)	17.33 (0.95)	17.81 (1.28)
V	21.09 (7.82)	21.15 (8.54)	21.24 (7.37)	21.36 (9.31)
Va	25.63 (4.54)	25.63 (4.92)	25.36 (4.27)	24.96 (5.73)
Vb				23.45 (3.58)
VI	27.18 (4.81)	27.11 (5.25)	27.08 (4.51)	26.27 (5.85)

[a] Band positions are given in $cm^{-1} \times 10^{-3}$. [b] Parenthesized intensities are extinction coefficients $\times 10^{-4}$.

Table II. Low-Wavenumber Resonance Raman Peak Positions and Assignments for Complexes **1a–d** in Tetrahydrofuran Solution with 476-nm Excitation

porphyrin				
[Mn(TPP)Cl]	[Mn(T(4-OCH_3P)P)Cl]	[Mn(T(4-ClP)P)Cl]	[Mn(T(4-CNP)P)Cl]	assgnt
113[a] (9.2)[b]	115 (12.2)	113 (17.2)	112 (10.7)	$\nu_{35}(B_{2g})$, dp,[c] δ(pyr trans)
201 (25.8)	166 (6.3)	160 (11.6)	170 (11.8)	$\varphi_{10}(A_{1g})$, p, $\nu(C_m\text{–Ph})$
	180 (2.0)	182 (4.6)		p
218 (8.1)	219 (8.9)	220 (10.6)	214 (24.7)	dp
240 (13.4)	*d*	*d*	241 (10.8)	$\nu_{13}(B_{1g})$, dp, $\delta(C_m\text{–Ph})$
258 (14.2)	242 (20.8)	247 (35.3)	260 (25.0)	$\gamma_7(A_{2u})$, p, $\gamma(C_\alpha\text{–}C_m)$
283 (5.0)	273 (4.5)	275 (9.0)	285 (5.5)	$\nu_{18}(B_{1g})$, dp, ν(Mn–N)
306 (11.7)	308 (13.8)	302 (8.4)	308 (5.9)	$\gamma_6(A_{2u})$, p, pyr tilt
		319[e] (14.5)		p
		339[e] (6.3)		dp
332 (11.2)	339 (5.7)	358 (21.5)	333 (13.7)	$\gamma_2(A_{1u})$, p, pyr swivel
394 (100.0)	387 (100.0)	381 (100.0)	385 (100.0)	$\nu_8(A_{1g})$, p, ν(Mn–N)
450 (2.0)	452 (2.2)	450 (4.2)		$\nu_{33}(B_{2g})$, dp, δ(pyr def)$_{sym}$
500 (2.2)	471 (3.1)	470 (13.9)		$\pi_4(\nu_4)(B_{1g})$, dp, phenyl oop

[a] Peak positions are given in relative wavenumbers. [b] Parenthesized values are peak heights relative to the dominant ν_4 mode. [c] Measured polarization characteristics; p = polarized, dp = depolarized. [d] This band is obscured by the strong overlapping band nearby. [e] The reason for the extra bands in the spectrum of **1c** and the intensity of the peak at 470 cm^{-1} is not well established. Work is continuing in this area.

the absorption bands typical of a manganese(III) porphyrin; however, the Q bands are shifted to higher energy and major changes in band intensity are observed in the region of bands V, Va, Vb, and VI. $[Mn(TPP)(L)_x]^+$ (**2a**) and its *p*-OCH_3 (**2b**) and *p*-Cl (**2c**) analogues have marked drops in intensities of band V, and for $[Mn(TPP)(L)_x]^+$ and $[Mn(T(4\text{-}OCH_3P)P)(L)_x]^+$, band Vb is a well-resolved peak. $[Mn(T(4\text{-}CNP)P)(L)_x]^+$ (**2d**) shows a trend opposite to that of the other samples with band V being considerably more intense in this spectrum than in the spectrum of [Mn(T(4-CNP)P)Cl] (**1d**). Also band Vb is significantly less well resolved and is observed as a shoulder on the low-energy side of band Va. Band positions and extinction coefficients for the dissociated metalloporphyrins also are given in Table I.

Resonance Raman Spectroscopy. Resonance Raman spectra of all four porphyrin samples (**1a–d**) were recorded over the range 50–1700 cm^{-1} in tetrahydrofuran (THF) and at concentrations of $Bu_4N^+BF_4^-$ from 0 to 0.5 M by irradiating into band V in each case; i.e., λ_{ex} = 476.5 nm. The high-wavenumber region of these spectra (1200–1700 cm^{-1}) exhibits the spin- and oxidation-state marker bands characteristic of manganese(III) porphyrins[33] as well as other porphyrin skeletal modes. The overall structure of the region is similar to other metalloporphyrins.[33,34] The low-wavenumber region of these spectra (50–500 cm^{-1}) is, however, different from that of most other metalloporphyrins. In each case, it is quite structured and there are notable differences between the spectra of the four samples (**1a–d**). A summary of the band positions, relative intensities, polarizations, and assignments for

(33) Parthasarathi, N.; Hansen, C.; Yamaguchi, S.; Spiro, T. G. *J. Am. Chem. Soc.* **1987**, *109*, 3865.
(34) Chottard, G.; Battioni, P.; Battioni, J.; Lange, M.; Mansuy, D. *Inorg. Chem.* **1981**, *20*, 1718.

Table III. Low-Wavenumber Resonance Raman Peak Positions and Assignments for Complexes **2a–d** in Tetrahydrofuran Solution with 476-nm Excitation

porphyrin				
$[Mn(TPP)]^+$	$[Mn(T(4\text{-}OCH_3P)P)]^+$	$[Mn(T(4\text{-}ClP)P)]^+$	$[Mn(T(4\text{-}CNP)P)]^+$	assgnt
123[a] (5.4)[b]	124 (5.3)	124 (5.6)	121 (6.4)	$\nu_{35}(B_{2g})$, dp,[c] δ(pyr trans)
202 (3.9)	165 (1.4)	160 (2.7)	168 (3.6)	$\varphi_{10}(A_{1g})$, p, $\nu(C_m\text{–Ph})$
240 (1.1)	238 (4.4)	239 (3.6)	240 (3.1)	$\nu_{13}(B_{1g})$, $\delta(C_m\text{–Ph})$
273 (2.1)		261 (5.8)		$\nu_{18}(B_{1g})$, ν(Mn–N)
332 (8.7)	338 (7.1)	358 (17.9)	333 (18.6)	$\gamma_2(A_{1u})$, p, pyr swivel
396 (100.0)	389 (100.0)	384 (100.0)	388 (100.0)	$\nu_8(A_{1g})$, p, ν(Mn–N)
	470 (5.0)	470 (23.5)		$\pi_4(\nu_4)(B_{1g})$, dp, phenyl oop

[a] Peak positions are given in relative wavenumbers. [b] Parenthesized figures are peak heights relative to ν_4. [c] Measured peak polarizations; p = polarized, dp = depolarized. Where no polarization is given, the peaks were too weak to measure depolarization ratios.

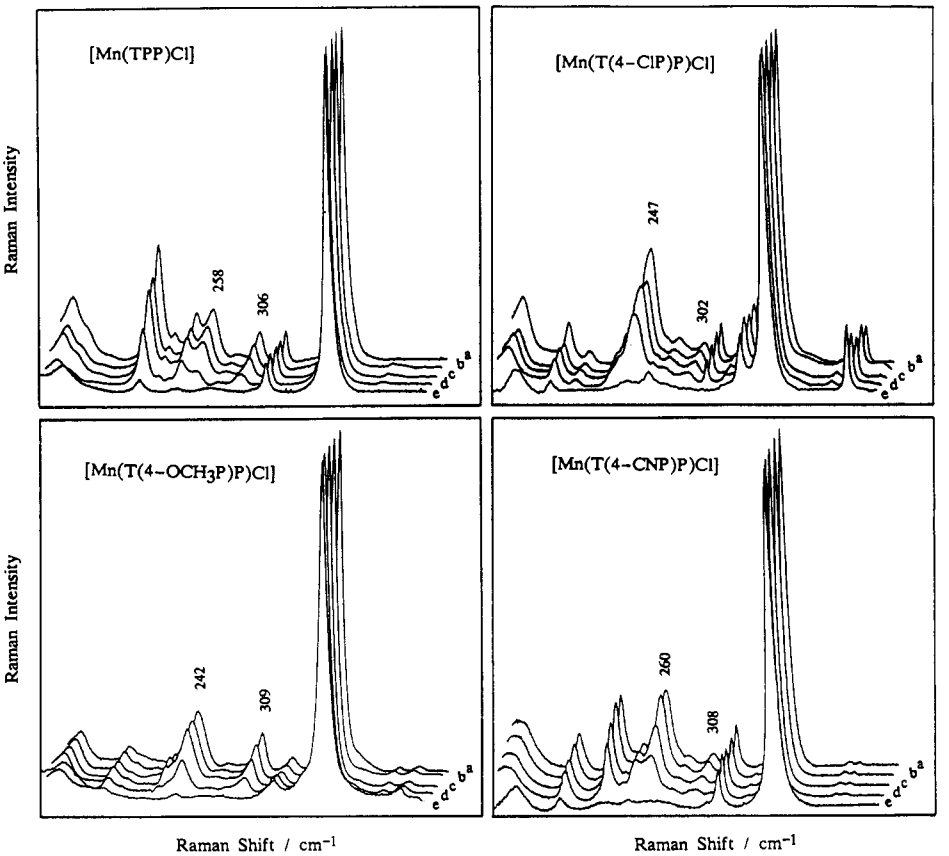

Figure 2. Effect of increasing $[Bu_4N^+BF_4^-]$ and chloride extraction on the low-wavenumber RR spectra of compounds **1a–d** in THF solution. Each spectrum covers the range 100–500 cm^{-1}. Concentrations of $Bu_4N^+BF_4^-$ are (a) 0.001 M, (b) 0.010 M, (c) 0.100 M, and (d) 0.500 M. (e) is the result of treating a THF solution of the metalloporphyrin with $AgBF_4$.

this region of the RR spectrum for the four metalloporphyrins (**1a–d**) is given in Table II.

The RR spectra also were recorded in THF solutions at concentrations of $Bu_4N^+BF_4^-$ from 0 to 0.5 M. Significant variations in band intensities were observed in the low-wavenumber region of each spectrum. Further, the RR spectra of the totally dissociated porphyrins (**2a–d**) were recorded. The most notable feature of these spectra is loss of structure in the low-wavenumber region. While the intense peak at about 380–395 cm^{-1} is relatively unchanged, most of the other modes have significantly decreased in relative intensity or disappeared completely (see Tables II and III). The variation in the RR spectra with varying $[Bu_4N^+BF_4^-]$ and after treatment with $AgBF_4$ is shown in Figure 2 for the four metalloporphyrins (**1a–d**). To determine which of the modes in the low-wavenumber region of the RR spectra are axial-ligand dependent in THF solution, the RR spectrum of a ^{37}Cl-substituted sample of complex **1a** was recorded simultaneously with that of the natural-abundance Cl-substituted complex using a split spinning cell and two-channel data collection. The spectrum of the natural-abundance Cl-substituted complex was then subtracted from that of the ^{37}Cl-substituted complex. This subtraction spectrum is shown in Figure 3. The bands at 256 and 306 cm^{-1} have shifted down by 2.0 and 1.5 cm^{-1}, respectively. Figure 4 shows the RR spectra of [Mn(TPP)Cl] and [Mn(TPP)Br] recorded in dichloromethane solution.

Electrochemistry. A typical linear sweep voltammogram of [Mn(TPP)Cl] obtained using the gold ultramicrodisk electrode is shown in Figure 5 with its second derivative as used to determine $E_{1/2}$ of the Mn(III/II) redox couple. Half-wave potentials of the Mn(III/II) couple were thus recorded for $[Bu_4N^+BF_4^-]$ ranging from 0.000 266 to 0.5 M and are quoted relative to the ferrocenium/ferrocene redox couple in Table IV. The potential of the Mn(III/II) couple is observed to shift quite markedly for [Mn(TPP)Cl] (**1a**) and $[Mn(T(4\text{-}OCH_3P)P)Cl]$ (**1b**) with the latter form being the most sensitive to variations in $[Bu_4N^+BF_4^-]$. [Mn(T(4-ClP)P)Cl] (**1c**) and [Mn(T(4-CNP)P)Cl] (**1d**) are less sensitive with much smaller shifts being observed. The broadness of the electrochemical responses (Figure 5) characterized the redox couple as being quasi-reversible.

The potentials of the Mn(III/II) redox couples of the anion-dissociated metalloporphyrin species (**2a–d**) were measured using a 1-mm gold disk electrode and cyclic voltammetry. These potentials are given in Table IV. It was not possible to measure this potential for compound **2d** (see Discussion), but the other three

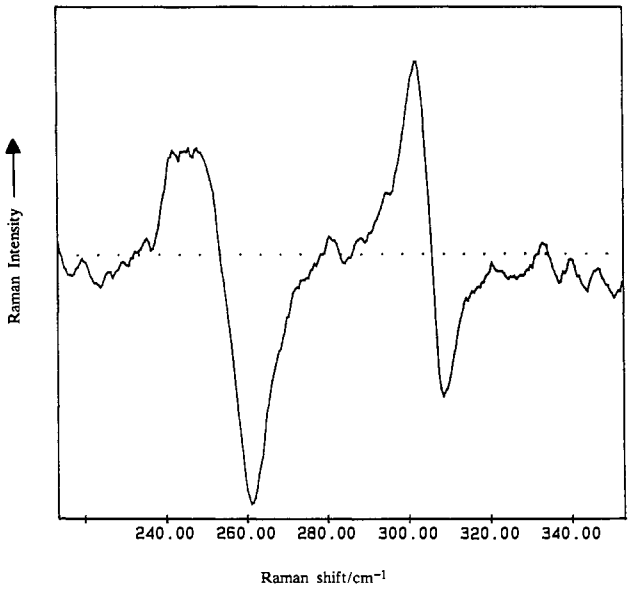

Figure 3. Resonance Raman spectrum obtained by subtracting the spectrum of [Mn(TPP)^{na}Cl] from that of [Mn(TPP)^{37}Cl] (na = natural abundance).

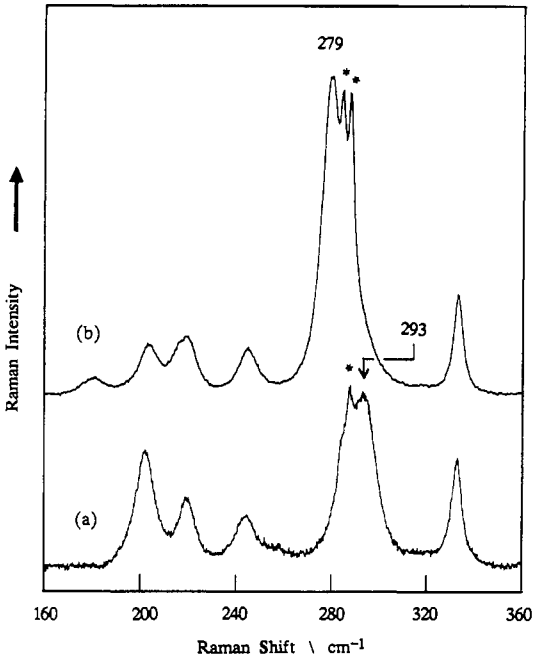

Figure 4. Resonance Raman spectra of (a) [Mn(TPP)Cl] and (b) [Mn(TPP)Br] in dichloromethane following excitation at 476 nm. The positions of the axial-ligand-dependent modes are given. Peaks marked with an asterisk are solvent bands.

Table IV. Dependence of the Mn(III/II) Redox Couple of Manganese(III) Tetraphenylporphyrin Chlorides on the Concentration of the Supporting Electrolyte

	half-wave potential of Mn(III/II) redox couple/mV[a]			
$[Bu_4N^+BF_4^-]$/M[b]	[Mn(TPP)Cl]	[Mn(T(4-OCH_3P)Cl]	[Mn(T(4-ClP)P)Cl]	[Mn(T(4-CNP)P)Cl]
0.000 266	−1027	−1064	−1255	−1113
0.001 179	−975	−1018	−1121	−1016
0.010 06	−906	−942	−1012	−906
0.100 5	−813	−842	−935	−899
0.505 7	−759	−765	−900	−935
0.100 0[c]	−644	−670	−583	

[a] All half-wave potentials are quoted relative to the ferrocenium/ferrocene redox couple. [b] $Bu_4N^+BF_4^-$ = tetrabutylammonium tetrafluoroborate. [c] This solution included an excess of $AgBF_4$ relative to the porphyrin sample.

values indicate that **2c** is the most readily reduced followed by **2a** and **2b**. The peak to peak separations in these scans were ~70 mV for **2a**, ~100 mV for **2b**, and ~140 mV for **2c**.

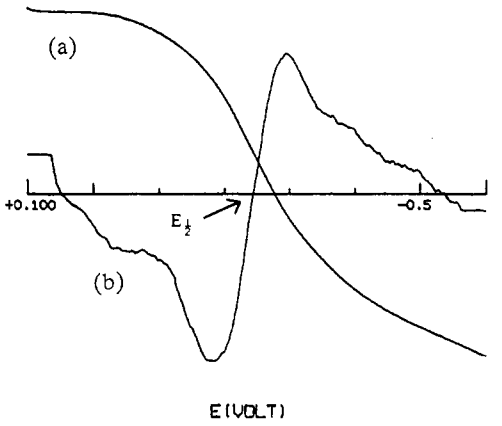

Figure 5. Typical linear sweep voltammogram (a) and its second derivative (b) for [Mn(TPP)Cl] obtained using a 10-μm gold microdisk electrode. The potential scale is relative to a Ag/AgCl/KCl(saturated) reference electrode which is at a potential of −643 mV versus Fc^+/Fc under these experimental conditions.

Discussion

Increasing the concentration of $Bu_4N^+BF_4^-$ has the effect of promoting dissociation of the axial chloride ligand in manganese(III) porphyrins **1a–d**. The sensitivity of the metalloporphyrins to this electrolyte-promoted axial-anion dissociation varies with the nature of the peripheral aryl substituent.

The changes that occur in the electronic absorption spectra on increasing the concentration of electrolyte (see Table I and Figure 1) indicate some perturbation of the electronic structure of the metalloporphyrins. The changes are enhanced in those solutions that have been treated with $AgBF_4$, as shown in the spectra of compounds **2a–d**. This process of chloride removal has previously been used to generate iron(III) porphyrin cations from the corresponding iron(III) chloride compounds.[35] In the present case the observation is consistent with the above interpretation that increasing concentrations of electrolyte are promoting the dissociation of axial chloride from the metalloporphyrin (i.e., the conversion of porphyrins **1a–d** to cations **2a–d**, respectively), the process being driven to completion by added Ag^+, affording insoluble AgCl as a byproduct. The resulting species was still a manganese(III) porphyrin as evidenced by the visible absorption spectrum, which, while showing significant variation and the previously unreported band Vb, still has the essential split-Soret character of a manganese(III) metalloporphyrin. Also, in the RR spectra of species **2a–d**, the oxidation-state marker band at ca. 1366 cm^{-1} is unshifted from its positions in the spectra of compounds **1a–d**.

Further evidence supporting this hypothesis is obtained from the effect of the peripheral phenyl substituents on the degree to which the concentration of $Bu_4N^+BF_4^-$ affects the visible spectrum. It would be expected that of the four metalloporphyrins (**1a–d**), the $-OCH_3$ and −H phenyl-substituted species would have the most weakly bound axial chloride owing to the relative electron-donating capacity of these substituents. The relatively higher electron density on the peripheral phenyl groups is communicated to the porphyrin, thus stabilizing the Mn(III) cation. Accordingly, these metalloporphyrins should show the greatest effect as $[Bu_4N^+BF_4^-]$ is increased. This is in fact what is observed (see Table I) with the visible spectrum at $[Bu_4N^+BF_4^-]$ = 0.5 M for **1a** and **1b** being more like that of the totally dissociated species (**2a,b**) than is the case for the −Cl- and −CN-substituted complexes, under the same conditions. For [Mn(T(4-ClP)P)Cl] and [Mn(T(4-CNP)P)Cl], where axial chloride binding is strongest, the effects of electrolyte on the spectra are small. All this is consistent with an interpretation in terms of axial chloride dissociation with increasing concentration of $Bu_4N^+BF_4^-$. The visible spectrum of compound

(35) Baldwin, J. E.; Haraldsson, G. G.; Jones, J. G. *Inorg. Chim. Acta* **1981**, *51*, 29.

2d shows trends quite different from those of the other three metalloporphyrins. We cannot at this stage offer an explanation for these unusual intensity variations; however, it is suspected that the peripheral cyano groups may be acting as ligands themselves to a neighboring metalloporphyrin molecule and so disrupt the electronic structure. The most striking feature of the electronic absorption spectra of compounds **2a–d** is the appearance of the new band labeled herein as band Vb. The absorption band shapes in the visible spectra of complexes **1a–d** suggest that this band may even be present when axial chloride is associated but with much lower molar extinction. The position of this band falls in the region that is usual for the Soret transition of other metalloporphyrins and may well be largely of this character. Also, the consistent shifts of the porphyrin Q bands to higher energy when going from species **1a–d** to their anion dissociated analogues is indicative of a perturbation of the normal porphyrin a_{1u},$a_{2u} \rightarrow e_g(\pi^*)$ electronic transitions. The direction of this shift is consistent with a lowering of the configuration interaction between the two transitions that give rise to the Soret and Q absorption bands as the axial anion is removed and the overlap of the manganese d-orbitals with those of the macrocycle π-system is enhanced. RR excitation profiles and low-temperature UV–vis experiments are currently being undertaken to elucidate further the electronic structure of these complexes.

While electronic absorption spectroscopy provides definite evidence of the concentration of $Bu_4N^+BF_4^-$ affecting the solution structures, and indirectly points to axial ligand dissociation, resonance Raman spectroscopy is a more powerful tool in determining the nature of the structural changes. The strong manganese–porphyrin interaction gives rise to a mechanism whereby the metal environment, in particular the axial ligands, can be probed by resonance Raman experiments. That is, excitation in the region of band V in these complexes results in a Raman spectrum from which is available not only information concerning the porphyrin skeleton but also details concerning metal–ligand bonding. The low-wavenumber region (50–500 cm^{-1}) of resonance Raman spectra of manganese(III) tetraarylporphyrins thus obtained contains some modes that are phenyl vibrations and others that are axial-ligand-dependent modes of the porphyrin skeleton.[19] It is also likely that some of the modes are porphyrin out-of-plane modes, as are observed in NiTPP.[36,37] The positions and assignments of axial-ligand-dependent modes have not been reported previously for THF solutions of manganese(III) tetraarylporphyrins. In the case of complex **1a**, the modes of the RR spectrum that are sensitive to the nature of the axial ligand have been determined by ^{37}Cl substitution. The subtraction spectrum (Figure 3) clearly shows shifts to lower energy in the positions of the peaks which are at 256 and 306 cm^{-1} when natural-abundance chloride is present. It is these same modes which show the most marked variation with increasing $[Bu_4N^+BF_4^-]$ (Figure 2). The decrease in intensity of these modes relative to others in the same region is consistent with the notion of axial chloride dissociation being promoted by an increase in electrolyte concentration.

The RR spectra of solutions treated with a stoichiometric excess of $AgBF_4$ were also recorded in an attempt to establish the characteristic features of the totally dissociated porphyrin complex. It was hoped that these spectra would show a further progression, for each porphyrin, from the series collected at different $[Bu_4N^+BF_4^-]$. The RR spectra of manganese(III) porphyrin solutions that have been treated with $AgBF_4$ show a total disappearance of the modes in the low-wavenumber region which were decreasing in intensity as $[Bu_4N^+BF_4^-]$ was increased. Therefore, it is reasonable to conclude that the solutions thus treated contain the totally dissociated $[Mn^{III}(TPP)]^+$ (**2a**) (or its THF-bound analogue $[Mn^{III}(TPP)(THF)_2]^+$) and that the solutions of increasing electrolyte concentrations contain both some associated and increasing proportions of the dissociation products.

On the basis of the above conclusions and in the light of recent work with NiTPP,[36,37] we propose assignments for modes in the low-wavenumber region of the spectra of complexes **1a–d**, and **2a–d**.

Two factors work synergistically to affect the RR spectra. They are (i) the chemical/electronic effects of changing the nature of the axial ligand, i.e., from chloride to THF, and (ii) the concomitant symmetry variation from C_{4v} to D_{4h} which occurs as two THF molecules are ligated and the manganese ion moves back into the plane of the porphyrin ring.

The chloride-dissociated species (**2a–d**) most likely has two coordinated THF molecules as is the case for a range of other oxygen-donor ligands.[39–42] Thus, they will have D_{4h} symmetry, very similar to that of NiTPP in solution. It would be expected, therefore, that any modes that are observable in a solution RR spectrum of NiTPP should be observable in this case. Further, the well-established strong interaction between the manganese(III) ion and the porphyrin macrocycle results in an unusual electronic structure, one result of which is the enhancement in the RR spectrum of many non-totally-symmetric vibrational modes, even when the excitation wavelength is not in the region of the porphyrin Q bands. Thus we have assigned all bands in the low-wavenumber RR spectra of complexes (**2a–d**) by analogy with Li et al., who carried out a normal-coordinate analysis on NiTPP.[36,37] These assignments are given in Table III. Due to the very low intensity of a number of the bands in question (particularly those in the 220–320-cm^{-1} range), it was not possible to determine accurately depolarization ratios for all bands. Thus, it was on the basis of position, shifts observed by varying the phenyl substituent, and where possible polarization characteristics that bands in the stated region were assigned.

Extending the above assignments to complexes **1a–d** is not a trivial exercise, as both the electronic and symmetry variations must be considered. Changes in the electronic absorption spectra of complexes **1a–d** in the region of RR excitation after axial chloride dissociation are significant. For complexes **1a–c**, the result is a considerable decrease in the extinction coefficient of band V. It could be postulated that the decrease in relative intensity of some modes in the RR spectrum upon treatment with $Bu_4N^+BF_4^-$ or $AgBF_4$ is due to electronic variations in the molecule, the result of which is that those modes no longer have an allowed enhancement mechanism. If this were the case, no inferences could be drawn regarding the solution structure of the molecule. It appears however, that this is not the case, as a study of the high-wavenumber region of complexes **1a–d** and **2a–d** indicates. In this region, even with RR excitation within the contour of band V, a number of totally symmetric and non-totally symmetric porphyrin skeletal modes are observed.[33] If in going from complexes **1a–d** to **2a–d** a significant change in RR enhancement mechanism was taking place, it would be expected to manifest itself in this region as a variation in relative intensities between the totally and non-totally symmetric modes as each class is enhanced by a different mechanism. No such consistent variation is observed, and thus, it is concluded that electronic effects are not the major cause of observed variations in the RR spectra but rather structural and symmetry changes around the manganese(III) ion.

Tentative assignments for the low-wavenumber RR spectra of compounds **1a–d** are given in Table II. The assignments are made according to the D_{4h} model as proposed for compounds **2a–d**. It should be noted that the formal symmetry for these species is C_{4v}, and the effects of this lower symmetry will be greatest on the modes involving molecular motions in the region of the central metal ion. Further, it is not surprising that there are some modes which are unassignable according to the D_{4h} scheme. Importantly,

(36) Li, X.; Czernuszewicz, R. S.; Kincaid, J. R.; Spiro, T. G. *J. Am. Chem. Soc.* **1989**, *111*, 7012.
(37) Li, X.; Czernuszewicz, R. S.; Kincaid, J. R.; Su, O.; Spiro, T. G. *J. Phys. Chem.* **1990**, *94*, 31.
(38) Benzonitrile binds strongly to gold via the nitrile group: Gao, P.; Weaver, M. J. *J. Phys. Chem.* **1985**, *89*, 5040.
(39) Hatano, K.; Anzai, K.; Iitaka, Y. *Bull. Chem. Soc. Jpn.* **1983**, *56*, 422.
(40) Hill, C. L.; Williamson, M. M. *Inorg. Chem.* **1985**, *24*, 2836.
(41) Hill, C. L.; Williamson, M. M. *Inorg. Chem.* **1985**, *24*, 3024.
(42) Williamson, M. M.; Hill, C. L. *Inorg. Chim. Acta* **1987**, *133*, 107.

however, all the observed modes in the D_{4h} scheme have analogous modes in the C_{4v} case.

The assignments of the A_{1g} and phenyl vibrations are quite straightforward. The bands of more interest though are the in-plane Mn–N stretches and the porphyrin out-of-plane (oop) modes. For porphyrin oop modes to be observed at significant intensities as they are in the RR spectra of compounds **1a–d**, the mechanism of activation must be considered. The most efficient and likely mechanism in this case is symmetry lowering. Deviations from planarity in the porphyrin ring, nonequivalent axial ligation, and out-of-plane displacement of the metal ion are all factors that can lead to the activation of porphyrin oop modes.[43] The two modes which were observed by isotopic substitution to be axial-ligand-dependent have been assigned as being A_{2u} oop modes, which are formally disallowed in D_{4h} symmetry, and are therefore not observed in complexes **2a–d**. In C_{4v} symmetry however, A_{2u} modes become A_1 modes which are both formally allowed and polarized, which is the case for these two modes. Further, an investigation of the eigenvectors[37] for γ_7 (258 cm^{-1} in **1a**) shows that it constitutes motion of the central metal ion which is perpendicular to the plane of the porphyrin ring. Such a mode would be significantly enhanced in the case, such as this, of a species where the metal ion is already displaced from the ring and axial ligation is nonequivalent. Similarly, γ_6 (306 cm^{-1} in **1a**) involves considerable doming of the porphyrin ring and metal displacement. Such motions are facilitated by the C_{4v} symmetry of species **1a–d**. It has been reported previously that in the case of manganese(III) etioporphyrin two bands in the RR spectrum show a shift upon isotopic substitution of the axial chloride.[21] On this basis, and also with the results from halide substitution experiments, one of these two bands was assigned as being a Mn–Cl stretching vibration. The spectra of the isotopically labeled species of Asher and Sauer[21] are noisy and unconvincing. Further, no attempt was made to do a spectral substraction which may have clarified the result. Indeed, even the stated shifts are significantly less than would be expected for a pure Mn–Cl vibration. Depending on whether the Mn(III) ion is considered to be stationary or free moving, the mode at 285 cm^{-1} would be expected to shift between 5.8 and 7 cm^{-1}. Even if we accept the reported shift of 4 cm^{-1}, it is not great enough to allow assignment of this mode as pure Mn–Cl stretch. In the same way, substitution of Cl^- with Br^- would be expected to yield a shift of the 285-cm^{-1} mode to somewhere between 190 and 232 cm^{-1}. The Mn–Br stretch is in fact reported at 245 cm^{-1}. Though this mode may well have Mn–X character, it is obviously coupled to at least one porphyrin vibration. The coupling is even greater in the case of [Mn(TPP)Cl], where the mode at 256 cm^{-1} shifts just 2.0 cm^{-1} after ^{37}Cl substitution. Also, the RR spectra of [Mn(TPP)Cl] and [Mn(TPP)Br] in dichloromethane (see Figure 4) show a shift of the axial-ligand-dependent mode from 293 cm^{-1} in the Mn–Cl case to only 279 cm^{-1} in [Mn(TPP)Br]. It is on this basis then that we have assigned the mode at 256 cm^{-1} (and analogous modes in the spectra of the phenyl-substituted MnTPP chlorides) as predominantly γ_7 in character and not as the Mn–Cl stretch, although there is little doubt that these modes are extensively coupled.

The large decrease in intensity of the assigned oop modes upon conversion to compounds **2a–d** can thus be interpreted as indicating a return to D_{4h} symmetry with equivalent axial ligation and the manganese ion in the porphyrin plane. The only mode assigned as an oop mode which persists in complexes **2a–d** is γ_2 (332 cm^{-1} in **1a**). This is expected given that this mode appears strongly in the RR spectrum of NiTPP with 514-nm excitation.[36] The in-plane Mn–N stretch (ν_8, A_{1g}) also is tuned by axial ligation and metal displacement as is evidenced by the 2–3-cm^{-1} shift to higher energy in each case when complexes **1a–d** are converted to **2a–d** respectively.

While RR spectroscopy provides a good qualitative probe of the nature of the metal–ligand environment in these metalloporphyrins, a technique that is more sensitive to the metal ion is electrochemistry. If, as was predicted from the electronic absorption and RR results, a change in ligation and metal position relative to the porphyrin ring was taking place with varying the concentration of background electrolyte, it would certainly manifest itself as a significant variation in the Mn(III/II) redox potential.

Due to the conductivity requirements of conventional electrochemistry and the low dielectric constant of THF,[8] it is not possible to record meaningful voltammograms in such a system at electrolyte concentrations less than ~0.1 M. Therefore, ultramicroelectrodes were employed in these studies. The very small currents obtained when using ultramicroelectrodes result in good quality, non-*iR*-(ohmic drop)-distorted voltammograms in THF even at submillimolar levels of background electrolyte.

While the problems of ohmic drop when measuring redox potentials versus electrolyte concentration can be largely overcome with ultramicroelectrodes, there remains in such experiments a difficulty in referencing the redox potentials to some absolute standard. Much of the porphyrin electrochemistry reported to date has been referenced to standard calomel (SCE) or silver/silver chloride (Ag/AgCl/KCl(saturated)) reference electrodes.[10-13] Such reference electrodes can be used satisfactorily for comparative work as long as electrolyte concentration, solvent, and cell configuration are all constant throughout a series of experiments. However, experiments that involve varying electrolyte concentrations have varying liquid junction potentials between the reference electrode compartment and that of the working electrode. This prevents meaningful comparisons of potentials measured at different electrolyte concentrations. Thus, throughout this work, all measured redox potentials are quoted relative to the Fc^+/Fc redox couple.

The variations in values of $E_{1/2}$ for the Mn(III/II) couples versus $[Bu_4N^+BF_4^-]$ are quite large (Table IV); particularly for the [Mn(TPP)Cl] and [Mn(T(4-OCH_3P)P)Cl] complexes. Both the magnitude and direction of such potential shifts are consistent with an increase in axial chloride dissociation as $[Bu_4N^+BF_4^-]$ increases, since it is expected to observe a shift in the value of the reduction potential to a more positive value following the removal of an anionic species from its coordination sphere. The observed shifts in the values of the Mn(III/II) redox potentials and their quasireversibilities can be interpreted in a number of ways with both kinetic and thermodynamic considerations being important in influencing both parameters in the case of the chlorometalloporphyrins. The quasireversibility of these complexes has been noted before[10,11] and is consistent with the equilibrium below being on the time scale of the electrochemical experiment. This aspect requires further attention.

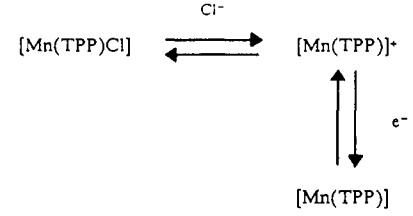

A further important point is the degree to which the measured half-wave potentials are affected by the substituents on the phenyl rings. The effect of phenyl ring substituents on the redox potentials of porphyrin ring oxidations and reductions have been previously reported for free-base and various metallotetraarylporphyrins.[27] These processes showed a linear free energy relationship between $E_{1/2}$ and the Hammett substituent constants for a number of phenyl substituents. The data for manganese(III) tetraarylporphyrins, however, are quite scant with only the first ring oxidation being reported reliably. The effect of such substituents on the metal redox couples is similarly unreported.

Given the strong interaction which exists between manganese(III) and the porphyrin ring, it would be expected that variations in the porphyrin electronic structure would be significantly communicated to the metal center and thus be observable in a

(43) Spiro, T. G.; Czernuszewicz, R. S.; Li, X. *Coord. Chem. Rev.* **1990**, *100*, 541.

study of the metal redox behavior.

If the variations in measured $E_{1/2}$ values for the Mn(III/II) couples are attributed to a change in the strength of binding of the axial chloride, then the differences between the metalloporphyrins at the same concentration of electrolyte are well explained in terms of the electron-donating/electron-withdrawing capacity of the phenyl ring substituents. That is, the porphyrin basicity is influenced by the phenyl substituents and is communicated to the manganese center. This affects the strength of the metal chloride bond and, thus, the tendency of chloride to stay associated as solution ionic strength is raised. Thus, for the -H- and $-OCH_3$-substituted samples, where electron-donating capacity is at its strongest, the largest variation in redox potential is observed with increasing $[Bu_4N^+BF_4^-]$ as the axial chloride is more readily removed. Further, at the same electrolyte concentrations, the -H and $-OCH_3$ phenyl-substituted samples have less negative values of $E_{1/2}$ for the Mn(III/II) redox couples relative to the -Cl- and -CN-substituted complexes, indicative of a greater degree of axial-anion dissociation. These redox potentials are influenced by both the degree of Cl^- association and the redox potential of the parent $[Mn(T(4\text{-}XP)P)]^{+/0}$ couple, where X represents the different phenyl substituents. The latter contribution is established from the redox potentials measured for the solutions which had been treated with a stoichiometric excess of $AgBF_4$. That is, the anion having already been removed, the -Cl-substituted sample has the least negative value of $E_{1/2}$ for Mn(III/II) owing to the greater electron-withdrawing capacity of the -Cl group. Similarly, the $-OCH_3$-substituted porphyrin has the most negative value for the reduction of the manganese ion as these substituents are most strongly electron donating and therefore have a stabilizing effect on the metal ion center with respect to reduction.

The above arguments account for the observed data for the -H, $-OCH_3$, and -Cl phenyl-substituted cases. The data for the -CN-substituted porphyrin, however, do not fit nicely into the same model. This substituent, is strongly electron withdrawing relative to the other three substituents, and therefore, $E_{1/2}$ values for the Mn(III/II) couple would be expected to be considerably more negative than for the other three complexes under identical conditions. That is, the axial chloride would be more resistant to dissociation given the more electropositive character of the metal ion bound to the porphyrin. However, this is not observed, and while the half-wave potentials of the Mn(III/II) couple are quite negative, they are no more so than those of the -Cl-substituted form under the same conditions. At the present time, no satisfactory explanation for this phenomenon is obvious. However, the behavior of the sample after being treated with $AgBF_4$ may provide some insight. No meaningful value for $E_{1/2}$ of the Mn(III/II) couple was obtainable for the -CN phenyl-substituted sample. All attempts to measure this were thwarted by a very large charging current in the region where the Mn(III/II) couple would be expected. This may be due to the cyano groups adsorbing onto the gold electrode and blocking the surface, thereby changing the character of the electrode.[38]

Conclusion

The present work investigates and quantifies the previously suggested notion that solution ionic strength can affect axial anion ligation in manganese(III) tetraphenylporphyrin chlorides. It is established that the effect is tuned by the peripheral phenyl substituents via a mesomeric interaction. This interpretation raises questions as to the reliability of previously reported electrochemical data which has been recorded using conventionally sized electrodes and electrolyte concentrations of at least 0.1 M. It also shows that carefully controlling the axial ligation may be a viable mechanism to tune the potentials of metal-centered redox couples in manganese porphyrins.

The electronic absorption and resonance Raman spectroscopic data for complexes **2a–d** are particularly intriguing, and work is continuing to further illucidate the electronic structure of these species.

The assignments of the low-wavenumber modes of the RR spectra highlight the sensitivity of, and the structural information that is available in, this much overlooked region of the RR spectrum.

Acknowledgment. We are grateful for assistance from Australian Research Council and the University of Sydney, Special Research Grants. We are also grateful for the assistance provided by Dr. Neale McAlpine in construction of ultramicroelectrodes and preamplifiers.

Registry No. **1a**, 32195-55-4; **1b**, 62769-24-8; **1c**, 62613-31-4; **1d**, 139312-20-2; **2a**, 139312-21-3; **2b**, 139312-22-4; **2c**, 139312-23-5; **2d**, 139312-24-6; tetrabutylammonium tetrafluoroborate, 429-42-5.